Materials Research Proceedings 41 (2024) 2226-2234 https://doi.org/10.21741/9781644903131-245

# Mechanical characterization and behavior modelling of Ti-6Al-4V alloy in hot forming conditions

D'ARCHIVIO Lucas[1,a*], PENAZZI Luc[1,b], VELAY Vincent[1,c], VIDAL Vanessa[1,d]

[1]Institut Clément Ader (ICA), Université de Toulouse, CNRS, IMT Mines Albi, INSA, UPS, ISAE-SUPAERO, UT3, Toulouse, France

[a]lucas.d_archivio@mines-albi.fr, [b]luc.penazzi@mines-albi.fr, [c]vincent.velay@mines-albi.fr, [d]vanessa.vidal@mines-albi.fr

**Keywords:** Behavior Modelling, Hot Forming, Ti-6Al-4V, Mechanical Testing, Digital Image Correlation (DIC)

**Abstract**. Ti-6Al-4V is a widely used titanium alloy in superplastic forming process which requires high temperatures ($\boldsymbol{T \approx 900\ °C}$) and low strain rates ($\boldsymbol{\dot{\varepsilon} \approx 10^{-3} s^{-1}}$). One way to reduce the costs of the process is to use a lower forming temperature and/or higher strain rate, up to $\boldsymbol{10^{-2} s^{-1}}$. However, the behavior of Ti-6Al-4V alloy still need to be modeled at such forming conditions and for different initial microstructure. In order to characterize the mechanical behavior of Ti-6Al-4V at temperature between 400 °C and 700 °C, relaxation and tensile tests performed under small and large deformation conditions were conducted. Depending on the test, the deformations were evaluated through two kinds of measurements, respectively with an extensometer and with a digital image correlation technique (DIC). Similar experimental results were obtained, validating the use of DIC at high temperature to evaluate high strain levels. Two different microstructures of Ti-6Al-4V alloy were tested to study the impact of the initial microstructure on the mechanical behavior. For similar conditions of strain rate and temperature, representative of the forming process, a fine-grained microstructure exhibits an enhancement of mechanical behavior in comparison with the classical coarse-grained microstructure used in the current industrial process. Finally, an elasto-viscoplastic has been identified for each microstructure.

## Introduction

Titanium alloys are widely used in the aerospace industry thanks to their high strength to weight ratio [1]. Titanium sheets are manufactured into parts for industrial applications by thermo-mechanical processes (heat treatment, machining, drilling, hot forming, …). These processes, along with the chemical composition of the alloy, can produce various microstructures which in turn influences the mechanical behavior. Therefore, a wide range of mechanical properties can be achieved for titanium alloys. One particular alloy stands out for aerospace application, the Ti-6Al-4V titanium alloy, an α + β alloy, used in critical parts of an airplane such as the engine. To shape it, a specific high temperature process is required to unlock its superplastic properties, the Superplastic Forming process (SPF). This process combines very high temperature ($\approx 900\ °C$) and low deformation rates ($\dot{\varepsilon} \approx 10^{-3} s^{-1}$) using inert gas punch to form parts with high level of deep-drawing. Its behavior has been well studied at room temperature [2] and at SPF temperatures [3]–[5]. To ensure lower energy consumption and faster processing time, some parts could be manufactured at lower temperature and higher strain rates in Hot Forming conditions (HF). Instead of a gas punch, this process makes use of a metallic punch to form the part. Some research have been made in that direction to explore the feasibility of forming Ti-6Al-4V alloy in such conditions [6], [7], by using numerical models to simulate the material behavior and the forming process, showing promising results.

Materials Research Proceedings 41 (2024) 2226-2234 https://doi.org/10.21741/9781644903131-245

Different types of model exist to describe the behavior of the Ti-6Al-4V alloy. They can be classified in a range from phenomenological to physical models. Johnson and Cook proposed a simple phenomenological model taking into account strain, strain-rates and temperature for several metals [8]. This model gives low stress discrepancy (~20 MPa) for room temperature and 400 °C [9], whereas Gao et al. results showed that the values of the parameters identified for 650 °C, 700 °C and 750 °C produces higher stress differences (~50 MPa in the best case) [10]. Physical models tries to integrates information about the microstructure, such as phase volume fraction, grain sizes [11], but also deformation mechanisms [5].

This study aims at characterizing and modelling the behavior of a Ti-6Al-4V titanium alloy at temperatures and strain rates for the HF process, i.e. from 400 °C to 700 °C and for strain rates up to $10^{-2}s^{-1}$. The behavior will be tested and modeled to high deformation levels using non-contact optical measurement of the strain by using Digital Image Correlation (DIC) in high temperature conditions. It will also explore the influence of the initial microstructure on the behavior by comparing two different microstructures.

## Material and methods

Materials description: two different microstructures of Ti-6Al-4V titanium alloy are studied in this paper. SEM micrographs showing the two microstructures are presented in Figure 1. The first microstructure is a Coarse Grained (CG) microstructure having equiaxed alpha nodules with an average grain size of 6 µm (Figure 1a) [6]. The second microstructure is a Fine Grained (FG) microstructure which is not fully equiaxed: the alpha phase is slightly elongated along RD and has an average grain size of 2 µm (Figure 1b) [12].

The CG and the FG microstructures are sampled from Ti-6Al-4V sheets having a thickness of respectively 1.7 mm and 3.2 mm. Their respective chemical composition is given in Table 1.

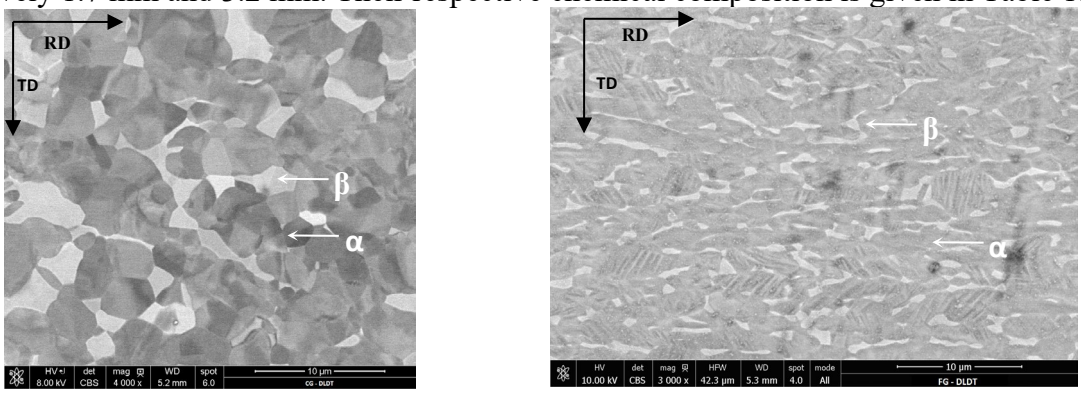


a) Coarse Grain microstructure (CG) b) Fine Grain microstructure (FG)

*Figure 1: SEM observations of the two initial microstructures (α phase in dark and β phase in white)*

*Table 1: Ti-6Al-4V alloy chemical composition for both microstructure*

| Microstructure | Ti | Al | V | Fe | O | C | N |
|---|---|---|---|---|---|---|---|
| FG [6] | Bal. | 6.26 | 3.92 | 0.24 | 0.33 | 0.01 | 0.01 |
| CG [12] | Bal. | 6.46 | 4.23 | 0.21 | 0.174 | 0.05 | 0.01 |

Procedure description: to characterize the mechanical behavior of the materials at several temperatures, two types of tests are performed on the Ti-6Al-4V alloy: a tensile relaxation test in small deformation to evaluate the elasto-viscoplastic behavior, and a tensile test to failure to upscale the model to large deformations calculated from a displacement field obtained using a DIC method.

For the relaxation test, the specimen is deformed to 0.02 deformation and relaxed for 30 min, deformation rate is set at $10^{-2}$ $s^{-1}$. The test is controlled by deformation using a contact extensometer, allowing a precise control over the deformation and deformation rate. 6 temperatures are tested, from 400 °C to 700 °C with the use of an AET furnace.

The second test is a tensile test under the same conditions of temperature where the specimen is deformed to rupture. Therefore, an extensometer cannot be used to measure the deformation in this case. Instead, a DIC method is implemented to acquire the displacement field between two images taken during the tests. In this study, logarithmic (Hencky) deformation is considered, and the software VIC-2D® is used for the DIC. In order to evaluate the displacement field, a speckle is applied on the surface of the specimen. A wide range of speckles specially developed for DIC can be found in the literature, from painting and laser marking to chemical etching and anodization [13]. For our test conditions, high temperature paints are used to ensure a resistant speckle even at 700 °C. To take account of the risk of the paint layer tearing due to the expected high deformation, no such layers are applied on the specimen. The paint is directly pulverized on the raw surface of the sample.

The samples are obtained by Water Abrasive Jet Cutting (WAJC) in the rolling direction, this study doesn't consider the anisotropy of the Ti-6Al-4V anisotropy.

**Experimental results**

Relaxation tests: the load and relaxation curves obtained for the FG microstructure are shown in Figure 2 for temperature levels between 400°C and 700°C. At 400 °C, the coarse-grained microstructure exhibits a stress 55 MPa higher than the fine-grained microstructure, due to a more pronounced hardening. However, at 600 °C, this gap falls to 10 MPa, and at 700 °C no difference in the stresses has been observed between the two microstructures at 0.02 strain level. It could indicate a similar mechanical response for both microstructures beyond 650 °C. At 650 °C and 700 °C, the stresses are fully relaxed before the 30 min holding time, which is not the case at lower temperatures.

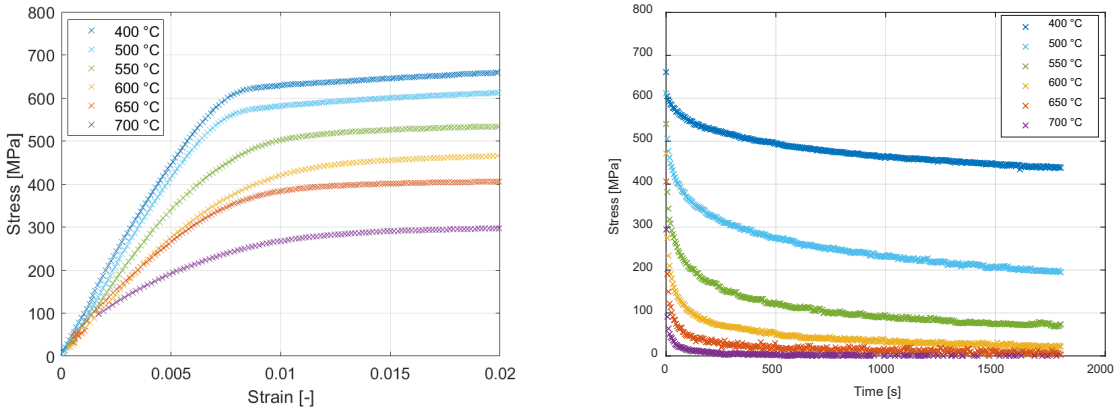


a) Load curves - FG b) Relaxation curves - FG

*Figure 2: Strain-Stress (a) and relaxation (b) curves for the FG microstructure*

Table 2 presents the elastic properties of the two microstructures, the Young's moduli E and the elasticity limits k. The latter are close to those reported by Luong et al. [14] who performed a measurement using a virtual extensometer based on DIC at high temperature. Other authors, such as Odenberger et al. [15], measured higher Young's modulus through an acoustic resonance analysis method (around 80 GPa at 700 °C). The elasticity limits presented Table 2 are estimated based on the method by Rollin et al. using the final stress during relaxation, minus the hardening [16]. For the elasticity limit, a Hall-Petch effect is present at the lower temperature, the fine-grained

microstructure having a higher elasticity limit than the coarse-grained one. Rollin reported an elasticity limit near zero for temperature higher than 650 °C with an initial 3 µm mean grain size Ti-6Al-4V alloy [16].

*Table 2: Young's modulus and elasticity limit evolution with temperature for the two microstructures*

| | CG | | FG | |
|---|---|---|---|---|
| Temperature [°C] | k [MPa] | E [GPa] | k [MPa] | E [GPa] |
| 400 | 250 | 94.1 | 300 | 98.2 |
| 500 | 80 | 87.1 | 100 | 89.1 |
| 550 | 30 | 70.8 | 40 | 69.7 |
| 600 | 5 | 64.9 | 10 | 57.6 |
| 650 | 0 | 50.8 | 0 | 54.1 |
| 700 | 0 | 39.9 | 0 | 33.6 |

Tensile tests: The strain-stress curves are presented in Figure 3. They were obtained by extracting the maximal deformation value from the deformation fields at each time increment. Each experimental point on the graphs is related to one image taken with the camera, and one deformation field. As the speckle deforms with the specimen, high deformation induces a severe decrease in the contrast of the speckle, almost deleting any speckle for the highest deformation value. When deformation reaches a value of about 2, errors in the DIC become too high and decorrelation occurs at the center of the necking area so the measurement cannot be done up to the rupture. Stress-strain values beyond that point should be carefully considered.

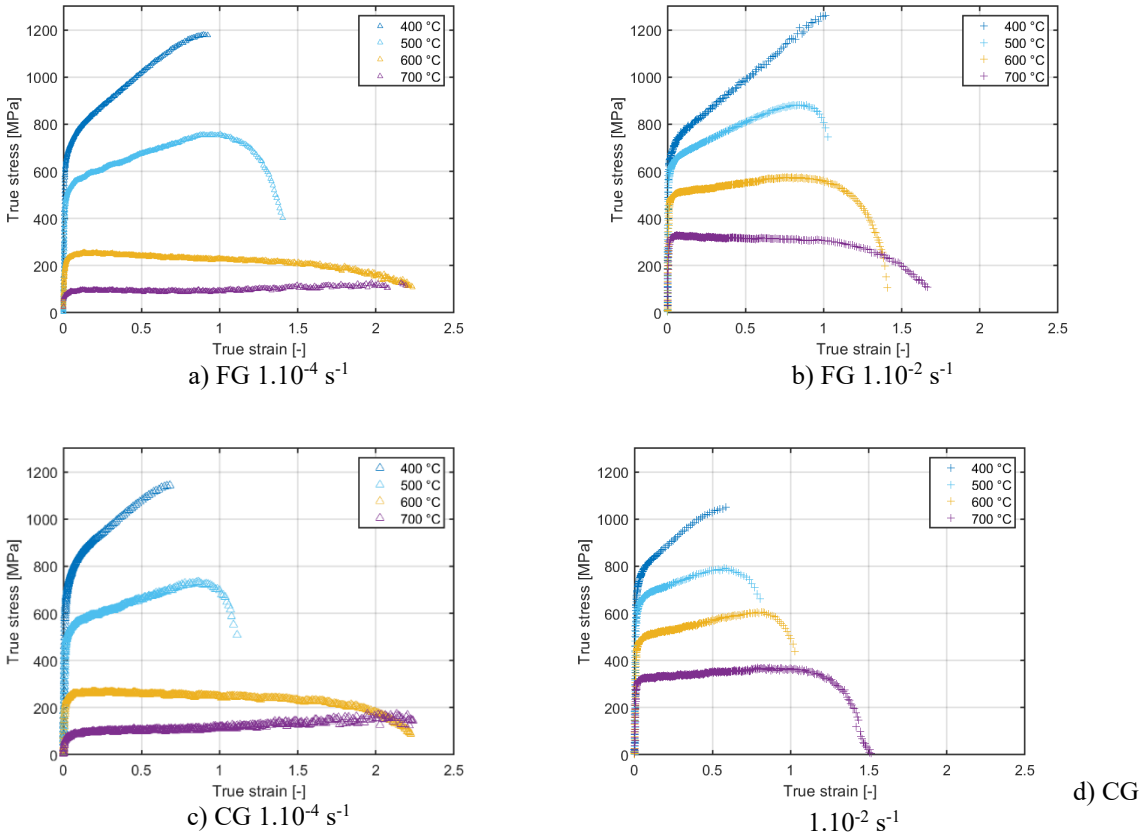


*Figure 3: Tensile strain-stress curves for all temperatures at $1.10^{-4}$ $s^{-1}$ (a, c) and $1.10^{-2}$ $s^{-1}$ (b, d) for the FG and CG microstructure*

Materials Research Proceedings 41 (2024) 2226-2234 https://doi.org/10.21741/9781644903131-245

For each combination of microstructure and deformation rate, an increase in temperature induces an increase in the strain at rupture and a decrease in true stress. The strain drops observed are not related to necking, but more likely to material damage. FG microstructure exhibits a higher deformation to rupture (Figure 4) and higher maximum stress in almost all cases compared to the coarse-grained microstructure. The viscoplastic effect activates for temperature starting at 500 °C for each microstructure, with no major impact at 400 °C. Strains at rupture between 0.92 and 1 were measured for the FG microstructure at 400 °C, whereas at 600 °C, a 0.8 strain difference between $1.10^{-2}$ $s^{-1}$ and $1.10^{-4}$ $s^{-1}$ has been evaluated. This difference is even higher considering that at $1.10^{-4}$ $s^{-1}$ a loss of correlation prevented the full acquisition of the strain level up to rupture.

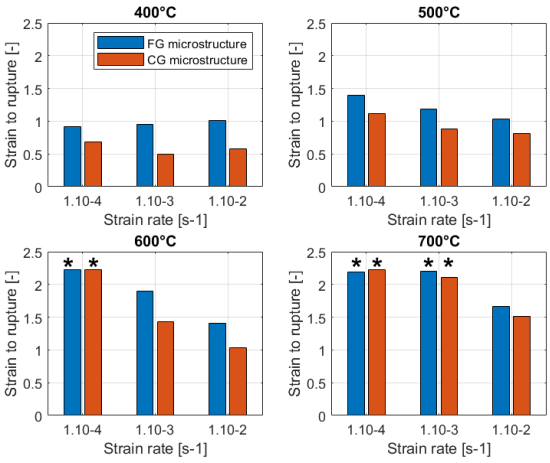


*Figure 4: Strain to rupture for all temperature, strain rate and both microstructure (* last strain measured before loss of correlation)*

Tensile-relaxation tests dialogue: the two campaigns generate experimental data in two different ways: through an extensometer for the relaxation tests and through DIC for the tensile tests. The concordance between the two campaigns has to be pointed out, particularly in the low deformation part. Figure 5 presents a comparison between the two kinds of tests, defined by the same loading path up to 0.02 deformation. The tensile curves measured by DIC shown here are slightly different from the ones shown in Figure 3b, as the deformation used here is a mean deformation in the whole region of interest instead of the maximum deformation value measured. This allows to be less sensitive on the noise and therefore to have smoother curves. This is further supported as there is no localization of the deformation at this strain. This method was not used in the Figure 5 as it underestimates the strain levels; For the FG microstructure, it lowers the strain at rupture by 0.21 at 400 °C and by 0.39 at 700 °C for a strain rate of $1.10^{-2}$ $s^{-1}$.

The two campaigns present close similarities even with two completely different means of measurement. This further validate DIC as a robust method to acquire deformation, at least for low strain.

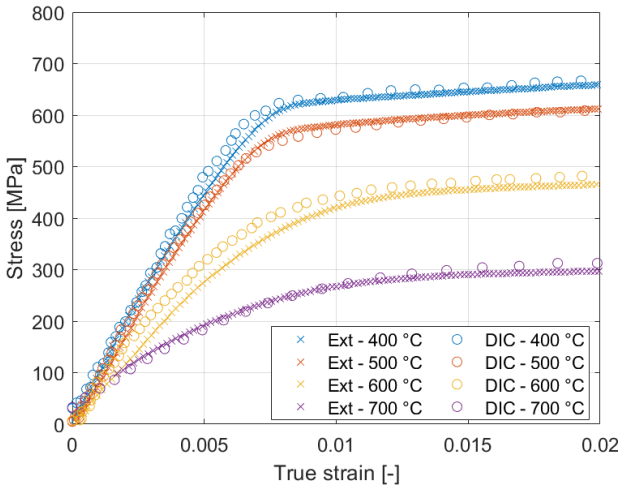


*Figure 5: Comparison between the two method of strain measurement: by extensometer and by DIC for the FG microstructure.*

**Material model**

Elasto-viscoplastic behavior: To model the behavior of the Ti-6Al-4V, an elasto-viscoplastic model is used. Strain-rate is partitioned between an elastic and a plastic strain-rate (Eq. 1). Elastic deformation is given according to Hooke's law (Eq. 2). The viscoplastic model chosen is a three-parameters hyperbolic sinus model (Eq. 3, Eq. 4). A two-parameter hardening law is used to describe the plasticity (Eq. 5). Finally, a von Mises yield surface mark the transition between elastic and viscoplastic deformation (Eq. 6).

$$\dot{\bar{\varepsilon}} = \dot{\bar{\varepsilon}}_e + \dot{\bar{\varepsilon}}_p \tag{1}$$

$$\dot{\bar{\sigma}} = \bar{\bar{C}}\dot{\bar{\varepsilon}}_e \tag{2}$$

$$\dot{\bar{\varepsilon}}_p = \frac{3}{2}\dot{p}\frac{\bar{s}}{\sigma_{eq}} \tag{3}$$

$$\dot{p} = Asinh(\beta f)^n \tag{4}$$

$$R = Q(1 - e^{-bp}) \tag{5}$$

$$f = \sigma_{eq} - k - R \tag{6}$$

**Model identification**

Method description: the Young's modulus and elasticity limit are identified from the tensile test performed under small deformation condition. In order to identify the 3 viscous parameters, Eq.7 is written as a log-log equation. The relaxation test is used to describe the evolution of the viscous stress and the viscoplastic strain rate is calculated as a function of the stress rate and the Young's modulus (Eq. 8).

$$\sigma_{vp} = \frac{1}{\beta} arcsinh\left[\left(\frac{1}{A}\left|\dot{\varepsilon_{vp}}\right|\right)^{\frac{1}{n}}\right] \tag{7}$$

Materials Research Proceedings 41 (2024) 2226-2234 https://doi.org/10.21741/9781644903131-245

$$\dot{\varepsilon_{vp}} = \frac{-\dot{\sigma}}{E} \quad (8)$$

Once the viscoplastic parameters have been identified, the last parameters to determine are the two hardening parameters. A first identification is done using the tensile test performed under small deformation conditions, up to 0.02 deformation.

**Results**

The evolutions of the 3 viscous parameters and the two hardening parameters with temperature is shown in Figure 6. Rollin et al. reported similar values and evolution for the viscous parameters [16]. The values of the hardening parameters b and Q (Figure 6b) show a decreasing evolution with temperature, the hardening is lower at higher temperature but also slower to reach its saturation value Q. The FG microstructure seems to present a higher hardening than the CG microstructure, at first contradicting the results of the relaxation tests. However, it should be considered that those hardening parameters identified give a faster saturation for the coarse-grained microstructure. No hardening is considered at 650 °C and above, and the parameters Q and b are set to 0. This identification does not yet include the traction to rupture test which, with higher strain levels, presents more hardening.

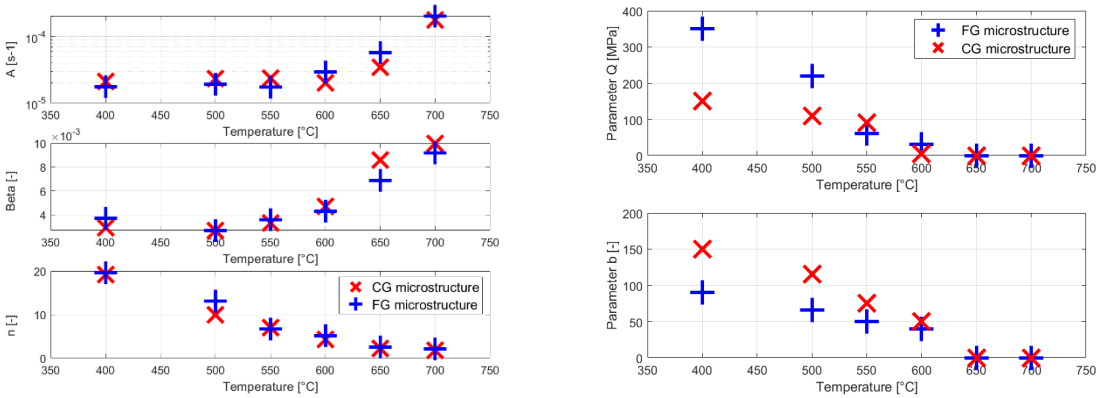


a) Viscous parameters b) Hardening parameters

*Figure 6: Model parameters evolution with temperature for both microstructures*

After identification of the viscoplastic part, a simple isotropic hardening was fitted to complete the model. A comparison between the experimental data and the modelling of the tensile curves for the FG microstructure is presented in Figure 7. The predicted stresses at 0.02 strain is consistent with the experimental stresses. More discrepancy exists at the onset of hardening, with a more abrupt elasto-viscoplastic transition for the model which predict higher stress, particularly at the low temperatures. The maximum gap between experimental and model is quantified according to Eq. 9. The values fluctuate around a 10% difference, mostly at the strain value of the elasto-viscoplastic transition for each temperature.

$$\sigma_{error} = \frac{|\sigma_{exp} - \sigma_{mod}|}{|\sigma_{exp}|} \quad (9)$$

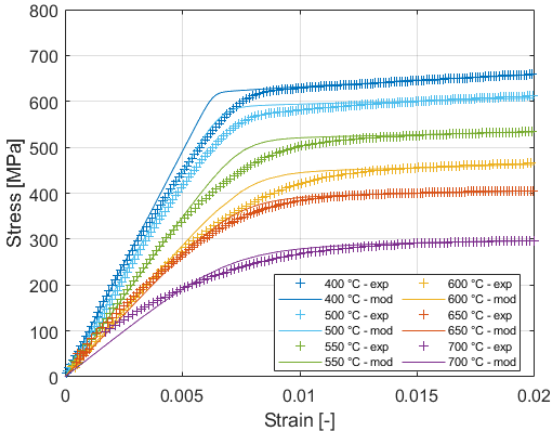


*Figure 7: Comparison between the experimental loading curves and the model at each temperature for the FG microstructure*

## Conclusion

This study investigated the mechanical behavior of two different microstructures of Ti-6Al-4V alloy at high temperature. The DIC method allowed to acquire information until very large strain (at least up to a true strain of 2) The results are in good agreement with the strain obtained using a contact method (extensometer).

An elasto-viscoplastic model has been identified using relaxation tests, under small strain condition. It presents a good agreement on the stress level, but still shows some mismatch near the elasto-viscoplastic transition.

The FG microstructure seems to show enhanced mechanical properties for forming processes compared to CG microstructure, with higher elongation at a given temperature and strain rate than the CG microstructure.

## Acknowledgment

The authors would like to begin by thanking the IMT Mines Albi engineering school and the Occitanie Region for financial aid towards this study ("Program: 00090414 / Folder: 21012548"). We would also like to offer special thanks to all the researchers and technicians in the ICA laboratories for their technical help and scientific advice.

## References

[1] Y. Combres, « Propriétés du titane et de ses alliages », *Métaux Alliages Non Ferr.*, août 2015. https://doi.org/10.51257/a-v1-m4780

[2] G. Gilles *et al.*, « Experimental characterization and elasto-plastic modeling of the quasi-static mechanical response of TA-6V at room temperature », *Int. J. Solids Struct.*, 48 (2011) 1277-1289. https://doi.org/10.1016/j.ijsolstr.2011.01.011

[3] N. Kotkunde, H. N. Krishnamurthy, P. Puranik, A. K. Gupta, et S. K. Singh, « Microstructure study and constitutive modeling of Ti–6Al–4V alloy at elevated temperatures », *Mater. Des.* 54 (2014) 96-103. https://doi.org/10.1016/j.matdes.2013.08.006

[4] L. Despax, « Étude des mécanismes de plasticité lors de la mise en forme de l'alliage de titane Ti-6Al-4V : influence de la microstructure initiale et des conditions de sollicitations thermomécaniques », Thesis, Ecole des Mines d'Albi-Carmaux, 2021. https://tel.archives-ouvertes.fr/tel-03579314

[5] R. Julien, V. Velay, V. Vidal, Y. Dahan, R. Forestier, et F. Rézaï-Aria, « Characterization and modeling of forged Ti-6Al-4V Titanium alloy with microstructural considerations during quenching process », *Int. J. Mech. Sci.*, 142-143 (2018) 456-467. https://doi.org/10.1016/j.ijmecsci.2018.05.023

[6] Q. Sirvin, « Etude du comportement mécanique de tôles en alliage de titane et des paramètres procédé dans les opérations d'emboutissage à hautes températures », Thesis, Ecole des Mines d'Albi-Carmaux, 2018.

[7] H. J. Bong, D. H. Yoo, D. Kim, Y.-N. Kwon, et J. Lee, « Correlative Study on Plastic Response and Formability of Ti-6Al-4V Sheets under Hot Forming Conditions », *J. Manuf. Process.*, 58 (2020) 775-786. https://doi.org/10.1016/j.jmapro.2020.08.053

[8] G. R. Johnson et W. H. Cook, « A Constitutive Model And Data For Metals », *Proc. 7th Int. Symp. Ballist.*, p. 541-547, 1983.

[9] N. Kotkunde, A. D. Deole, A. K. Gupta, et S. K. Singh, « Comparative study of constitutive modeling for Ti–6Al–4V alloy at low strain rates and elevated temperatures », *Mater. Des.*, 55 (2014) 999-1005, doi: 10.1016/j.matdes.2013.10.089

[10] S. Gao, Y. Sang, Q. Li, Y. Sun, Y. Wu, et H. Wang, « Constitutive modeling and microstructure research on the deformation mechanism of Ti-6Al-4V alloy under hot forming condition », *J. Alloys Compounds*, 892 (2022) 162128. https://doi.org/10.1016/j.jallcom.2021.162128

[11] P. Gao, M. Fu, M. Zhan, Z. Lei, et Y. Li, « Deformation behavior and microstructure evolution of titanium alloys with lamellar microstructure in hot working process: A review », *J. Mater. Sci. Technol.*, 39 (2020) 56-73. https://doi.org/10.1016/j.jmst.2019.07.052

[12] L. Despax, V. Vidal, D. Delagnes, M. Dehmas, H. Matsumoto, V. Velay, « Influence of strain rate and temperature on the deformation mechanisms of a fine-grained Ti-6Al-4V alloy », *Mater. Sci. Eng. A*, 790 (2020) 139718. https://doi.org/10.1016/j.msea.2020.139718

[13] P. Luong, R. Bonnaire, J. Périé, Q. Sirvin, et L. Penazzi, « Speckle pattern creation methods for two-dimensional digital image correlation strain measurements applied to mechanical tensile tests up to 700°C », *Strain*, 57 (2021) e12388. https://doi.org/10.1111/str.12388

[14] L. P. Luong, « Development of the two-dimension Digital Image Correlation method (2D-DIC) at high temperatures applicable for titanium alloys forming process », Thesis, Ecole des Mines d'Albi-Carmaux.

[15] E.-L. Odenberger, R. Pederson, et M. Oldenburg, « Finite element modeling and validation of springback and stress relaxation in the thermo-mechanical forming of thin Ti-6Al-4V sheets », *Int. J. Adv. Manuf. Technol.*, 104 (2019) 3439-3455. https://doi.org/10.1007/s00170-019-04071-9

[16] M. Rollin, « Study and Optimization of Cooling Conditions of Titanium Alloy Parts Manufactured by Superplastic Forming », Thèse, Ecole des Mines d'Albi-Carmaux, 2021.